N. Zotov

Heavy quark production with BFKL and CCFM dynamics

in collaboration with

S.P. Baranov (LPI, Russia)
H. Jung, L. Jonsson (Lund Univ., Sweden)
S. Padhi (McGill Univ., Canada)

In the framework of the semihard (k_T-factorization) approach we analyse the charm production processes at HERA.

B.A.

Bo Andersson et al
hep-ph/0204115

Content

Supplement

1. Introduction

Why **SHA**?

1) At **HERA** energy and beyond the **H.Q.** production – semihard process.
   By definition in these processes we have a hard scattering scale μ

$$\mu^2 \sim p_T^2 \sim M_T^2 = M^2 + p_T^2, \; M \sim M_Q$$

which is large as compared to the Λ_{QCD} parameter but μ is much less than the total c.m.s. energy $\sqrt{S}$ of a process

$$\Lambda_{QCD} \ll \mu \ll \sqrt{S}.$$

In such case $M^2/S \sim x \ll 1$ and we have deal with hard processes in small x region.

2) It means the **pQCD** expansion any observable quantity in α_S contains large coefficients $O(\ln^n(s/M^2)) \sim O(\ln^n(1/x))$ (besides the usual R.G. ones $O(\ln^n(\mu^2/\Lambda_{QCD}^2))$), which compensate the smallness of the coupling constant $\alpha_S(\mu^2/\Lambda_{QCD}^2)$.
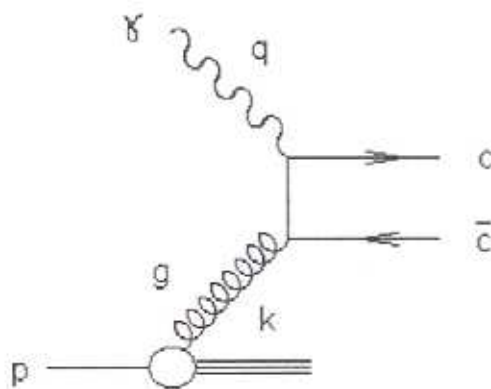
It is known the resummation of these terms $(\alpha_S \ln(1/x))^n$ (~ 1 at $x \to 0$) results in the so called unintegrated parton distributions $F_i(x, \vec{k}_T^2)$ ($k = xp + k_T$, $k_T^2 = -\vec{k}_T^2$) – the probability to find a parton carring the longitudinal momentum fraction x and transverse momentum k_T.

If the terms $(\alpha_S \ln(\mu^2/\Lambda_{QCD}^2))^n$ and **DL** terms $(\alpha_S \ln(\mu^2/\Lambda_{QCD}^2)\ln(1/x))^n$ are also resummed, then the unintegrated parton distributions **(u.p.d.)** depends also on the probing scale μ:

$$A(x, \vec{k}_T^2, \mu^2)$$

The **u.p.d.** obey certain evolution equations:

- **BFKL:** E.Kuraev, L. Lipatov, V. Fadin (1976, 1977); Yu. Balitsky, L. Lipatov, Sov. J. NP **28** (1978) 822.

- **CCFM:** M. Ciafaloni (1988); S. Catani, F. Fiorani, G. Marchesini (1990); G. Marchesini, NP **B445** (1995) 49.

u.p.d. are related to the conventional **DGLAP** densities once the k_T dependence is integrated out.

For example, the **u.g.d.** reduce to the conventional gluon density by

$$\int_0^{Q^2} F_g\left(x, \vec{k}_T^2\right) d\vec{k}_T^2 \simeq xG\left(x, Q^2\right).$$

3) LO+NLO calculations for heavy quark production have some **problems:**

- $\gamma p \to D^* X$, $ep \to e' D^* X$:
  all **pQCD** calculations underestimate total cross section at intermediate $p_T(D^*)$ and forward $\eta(D^*)$.

- $p\bar{p} \to b\bar{b} X$:
  all **pQCD** calculations underestimate total cross section also.

- $p\bar{p} \to J/\Psi X$, $p\bar{p} \to \Psi' X$, $p\bar{p} \to \chi_c X$:
  the very large disperanse (by more than an order of magnitude) between the **pQCD** predictions **(with CSM)** and existing experimental data at **TEVATRON**.

- **To reproduce the heavy quark transverse momentum spectra:** one usually introduces the promordial k_T of initial partons; the size of this k_T cannot be predicted within model itself and is required to be $k_T \sim 1-2$ **GeV** (instead k_T of the order $\Lambda_{QCD} \sim 300$ **MeV**) to fit the data.

$\Rightarrow$ We need the k_T-factorization approach **(SHA)**.

: L. Gribov, E. Levin, M. Ryskin, Phys. Reports C 100 (1983) 1

LRSS, Sov. J. NP 53 (1991) 657

and

J. Collins, R. Ellis, N.P. B360 (1991) 3
S. Catani, M. Ciafaloni, F. Hautmann, NP B366 (1991) 135

We used so called k-factorization

S. Catani, M.Ciafaloni, F. Hautmann, NP., **B366** (1991) 135; J. Collins, R. Ellis, NP., **B360** (1991) 3.

or semihard QCD approach

E. Levin, M. Ryskin, Yu. Shabelsky, A. Shuvaev, Sov. J. NP., **53** (1991) 657; L. Gribov, E. Levin, M. Ryskin, PR., **C100** (1983) 1.

We have used semihard QCD approach **(SHA)** earlier to describe experimental data on:

✓ heavy quark photoproduction $\gamma p \to Q\overline{Q} X$

V.A. Saleev, N.P. Zotov, MPL., **A11** (1996) 25; A.V. Lipatov, V.A. Saleev, N.P. Zotov, MPL., **A15** (2000) 1727.

✓ J/Ψ photoproduction $\gamma p \to J/\Psi X$

V.A. Saleev, N.P. Zotov, MPL., **A9** (1994) 151; A.V. Lipatov, N.P. Zotov, MPL., **A15** (2000) 695.

✓ D* electroproduction $ep \to e'D*X$

S.P. Baranov, N.P. Zotov, PL., **B458** (1999) 389); S.P. Baranov, N.P. Zotov, PL., **B491** (2000) 111.

✓ charm contribution to the proton structure function $F_2^c(x, Q^2)$, F_L^c, F_L

A.V. Kotikov, A.V. Lipatov, G. Parente, N.P. Zotov, hep-ph/0107135.

∨ $b\bar{b}$-production in $p\bar{p} \to b\bar{b} X$ at TEVATRON
A.V. Lipatov, V.A. Saleev, N.P. Zotov, hep-ph/0112114

∨ J/Ψ production in DIS with CSM and COM.
A.V. Lipatov, N.Z. hep-ph/020823
S.P. Baranov, N.Z.

2. <u>Unintegrated gluon distributions.</u>

We have used three different representation of the k_T dependent (unintegrated) **g.d.** $A(x, \vec{k}_T^2, \mu^2)$. One **(JB)** coming from a leading-order perturbative solution of the **BFKL** equation.

<u>JB</u>: J. Blumlein, DESY 95-121.

The second set **(JS)** derived from a numerical solution of the **CCFM** equation.

<u>JS</u>: H. Jung, hep-ph/9908497;
H. Jung, G. Salam, Eur. Phys. J. **C19** (2001) 351,
hep-ph/0012143.

The third **(KMR)** derived from solution of a combination of the **BFKL** and **DGLAP** equations.

<u>KMR</u>: M. Kimber, A. Martin, M. Ryskin,
PR **D63** (2001) 114027.

- **JB:** The unintegrated gluon density $A(x, \vec{k}_T^2, \mu^2)$ is calculated as a convolution of the ordinary gluon density $xG(x, \mu^2)$ (here we used **GRV** set) with universal weight factors:

$$A\left(x, \vec{k}_T^2, \mu^2\right) = \int_x^1 \phi\left(\eta, \vec{k}_T^2, \mu^2\right) \frac{x}{\eta} G\left(\frac{x}{\eta}, \mu^2\right) d\eta$$

$$\phi\left(\eta, \vec{k}_T^2, \mu^2\right) = \begin{cases} \dfrac{\overline{\alpha}_s}{\eta \vec{k}_T^2} J_0\left(2\sqrt{\overline{\alpha}_s \ln(1/\eta)\ln\left(\mu^2/\vec{k}_T^2\right)}\right), & \vec{k}_T^2 \leq \mu^2 \\[2ex] \dfrac{\overline{\alpha}_s}{\eta \vec{k}_T^2} I_0\left(2\sqrt{\overline{\alpha}_s \ln(1/\eta)\ln\left(\vec{k}_T^2/\mu^2\right)}\right), & \vec{k}_T^2 \geq \mu^2 \end{cases}$$

where $\overline{\alpha}_s = 3\alpha_s/\pi$, $\Delta = j - 1 = \overline{\alpha}_s 4 \ln 2 \sim 0.53$ in **LO** and $\Delta = \overline{\alpha}_s 4 \ln 2 - N\overline{\alpha}_s^2$ in **NLO**. In our calculations presented here we use the solution of the **LO BFKL** equation and treat Δ as free parameter varying between $0.166 \leq \Delta \leq 0.53$ with a central value of $\Delta = 0.35$.

U.g.d. $A(x, \vec{k}_T^2, \mu^2)$ is the first ingredient of **SHA**.

Second ingredient of **SHA** is off mass shell **m.e.** for **QCD** boson-gluon fusion subprocess $\gamma^* g^* \to Q\overline{Q}$, $Q = c, b$ with the modification of the gluon spin density matrix in **BFKL** form:

$$G^{\mu\nu} = \overline{\varepsilon_g^\mu \varepsilon_g^\nu} = \frac{k_T^\mu k_T^\nu}{\vec{k}_T^2}.$$

for photon polarization matrix in **DIS** we used

$$L^{\mu\nu} = \overline{\varepsilon_\gamma^\mu \varepsilon_\gamma^\nu} = 4\pi\alpha \frac{1}{(q^2)^2} \left(8 p_e^\mu p_e^\nu - 4(p_e q) g^{\mu\nu} \right)$$

So in **SHA** the hard $Q\overline{Q}$-electroproducion cross section is a convolution of the partonic boson-gluon fusion **c.s.** with k_T dependent (unintegrated) gluon density

$$\sigma = \int d\vec{k}_T^2 \, dx \, A\left(x, \vec{k}_T^2, \mu^2 \right) \hat{\sigma}\left(x, \vec{k}_T^2; \gamma^* g^* \to Q\overline{Q} \right)$$

with the off-shell **m.e.** either given by

- **CE-CCH**: J. Collins, R. Ellis, NP **B360** (1991) 3; S. Catani, M. Ciafaloni, F. Hautmann, NP **B366** (1994) 135.
- **SZ**: V. Saleev, N. Zotov, MPL **A11** (1996) 25.
- **BZ**: S. Baranov, N. Zotov, PL **B458** (1999) 389, PL **B491** (2000) 111, where the method of orthogonal amplidutes was applied R. Prange, PR **110** (1958) 240.

Since it is difficult to compare the different **m.e.** with each other analytically we have performed several numerical checks.

The results of **CE-CCH** and **SZ** agree prefectly. A systematic diference of the order of **10%** to the calculation of **BZ** is observed. It is effect of the "small x approximation" (Sudakov decomposition) at **HERA** energy.

- **JS:** The **CCFM** evolution equations have been solved numerically using a Monte-Carlo method.

  According to the **CCFM** evolution equations, the emission of partons during the initial cascade is only allowed in an angular-ordered region of phase space. The maximum allowed angle Ξ for any gluon emission sets the scale μ for the evolution and is defined by the hard scattering quark box, which connects the exchanged gluon to the virtual photon.
  The free parameters of the starting gluon distribution were fitted to the function $F_2(x, Q^2)$ in the range $x < 10^{-2}$ and $Q^2 > 5\,\mathrm{GeV}^2$, resulting in the **JS** unintegrated gluon distribution $xA(x, \vec{k}_T^2, \mu^2)$.

- **KMR:** In **KMR** the dependence of the unintegrated gluon distribution on the two scales k_T and μ was investigated: the scale μ plays a dual role, it acts as the factorization scale and also controls the angular ordering of the partons emitted in the evolution.

  This result in a form similar to the differential form of the **CCFM** equation, however the splitting function $P(z)$ is taken from the single scale evolution of the *unified* **DGLAP-BFKL** expression. The unintegrated gluon density $xA(x, \vec{k}_T^2, \mu^2)$ covering the whole range in k_T^2:

$$
xA\!\left(x, \vec{k}_T^2, \mu^2\right) =
\begin{cases}
\dfrac{1}{k_{T0}^2}\, xG\!\left(x, k_{T0}^2\right), & \text{if } k_T^2 < k_{T0}^2 \\[2ex]
\dfrac{1}{k_T^2}\, f\!\left(x, k_T^2, \mu^2\right), & \text{if } k_T^2 > k_{T0}^2
\end{cases},
$$

with $xG(x, k_{T0}^2)$ being the integrated **MRST** gluon density function and $f(x, k_T^2, \mu^2)$ being the unintegrated gluon density starting from $k_T > k_{T0} = 1\,\mathrm{GeV}$. The unintegrated gluon density $xA(x, \vec{k}_T^2, \mu^2)$ therefore is normalized to the **MRST** function when integrated up to k_{T0}^2.

3. Results

3.1 Transverse momentum distribution of D^* mesons: comparison of parton and hadron level

One observable which is expected to show only little sensitivity to the hadronization and to the full simulation of the initial and final state QCD cascades is the transverse momentum p_t of the D^* meson in photo-production and deep inelastic scattering. In Fig. 3 we show the
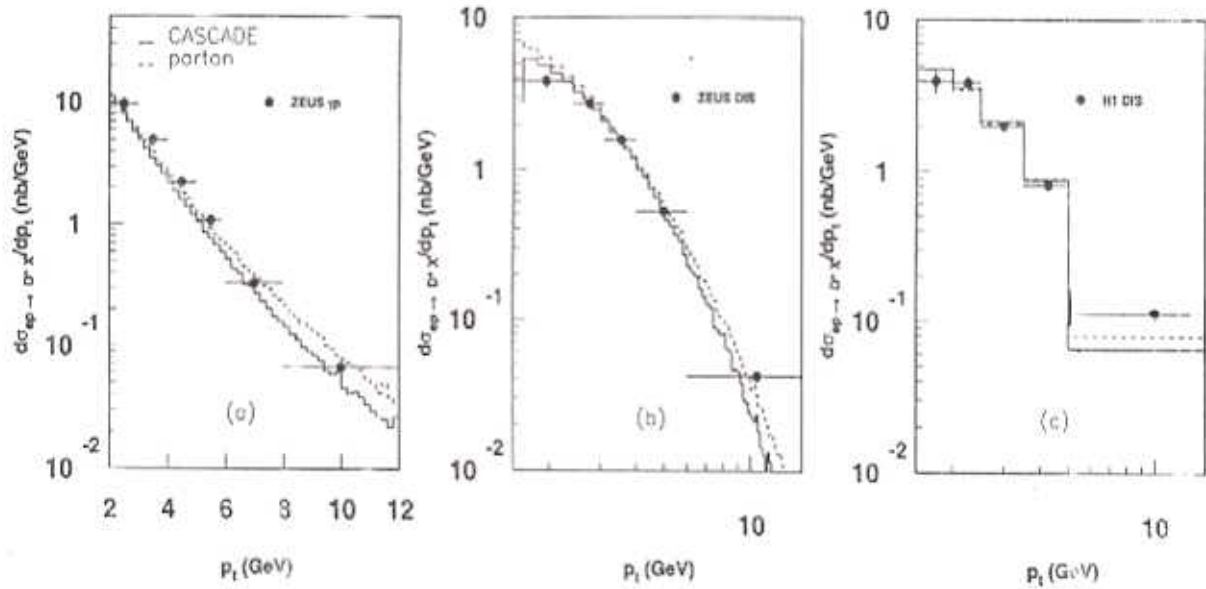

Figure 3: *The differential cross section $d\sigma/dp_t$ for D^* production: (a) in photo production (ZEUS [44]), (b) in DIS (ZEUS [45]) and (c) in DIS (H1 [46]). The solid line is the prediction from the full hadron level simulation CASCADE and the dashed line shows the parton level calculation. In both cases the Peterson fragmentation function has been used.*

transverse momentum distribution of D^* mesons as measured by the ZEUS [44,45] and H1 [46] collaborations both in photo-production and deep-inelastic scattering. The data are compared to the predictions of the CASCADE Monte Carlo event generator on hadron level including a full simulation of the partonic and hadronic final state. Also shown is the pure parton level calculation using the matrix element of BZ. In both cases the transition from the charm quark to the observed D^* meson was performed by a simple Peterson fragmentation function (with $\epsilon = 0.06$ and a $c \to D^*$ branching ratio $BR = 0.26$). The scale $\bar{\mu}^2$ in $\alpha_s(\bar{\mu}^2)$ was set to $\bar{\mu}^2 = p_t^2 + m_c^2$ with p_t being the transverse momentum in the γg cms of the final charm quark state assuming $m_c = 1.5$ GeV. The JS unintegrated gluon distribution [23] was used, with the scale μ related to the maximum angle $\mu^2 \sim x_\gamma x_g s$. The sensitivity to the details of the charm fragmentation and to the full initial state gluon cascade simulation can be seen by comparing CASCADE with the parton level calculation. We observe, that the p_t distribution of D^* mesons both in photo-production and deep inelastic scattering is in general well described, both with the full hadron level simulation as implemented in CASCADE and also with the parton level calculation supplemented with the Peterson fragmentation function. We can thus conclude, that the p_t distribution is only little sensitive to the details of the charm fragmentation.

8

In Fig. 2 we show a comparison of the gluon density distributions at $\overline{\mu}^2 = 100$ GeV^2 obtained from JB, JS and KMR as a function of x for different values of k_t^2 and as a function of k_t^2 for different values of x.
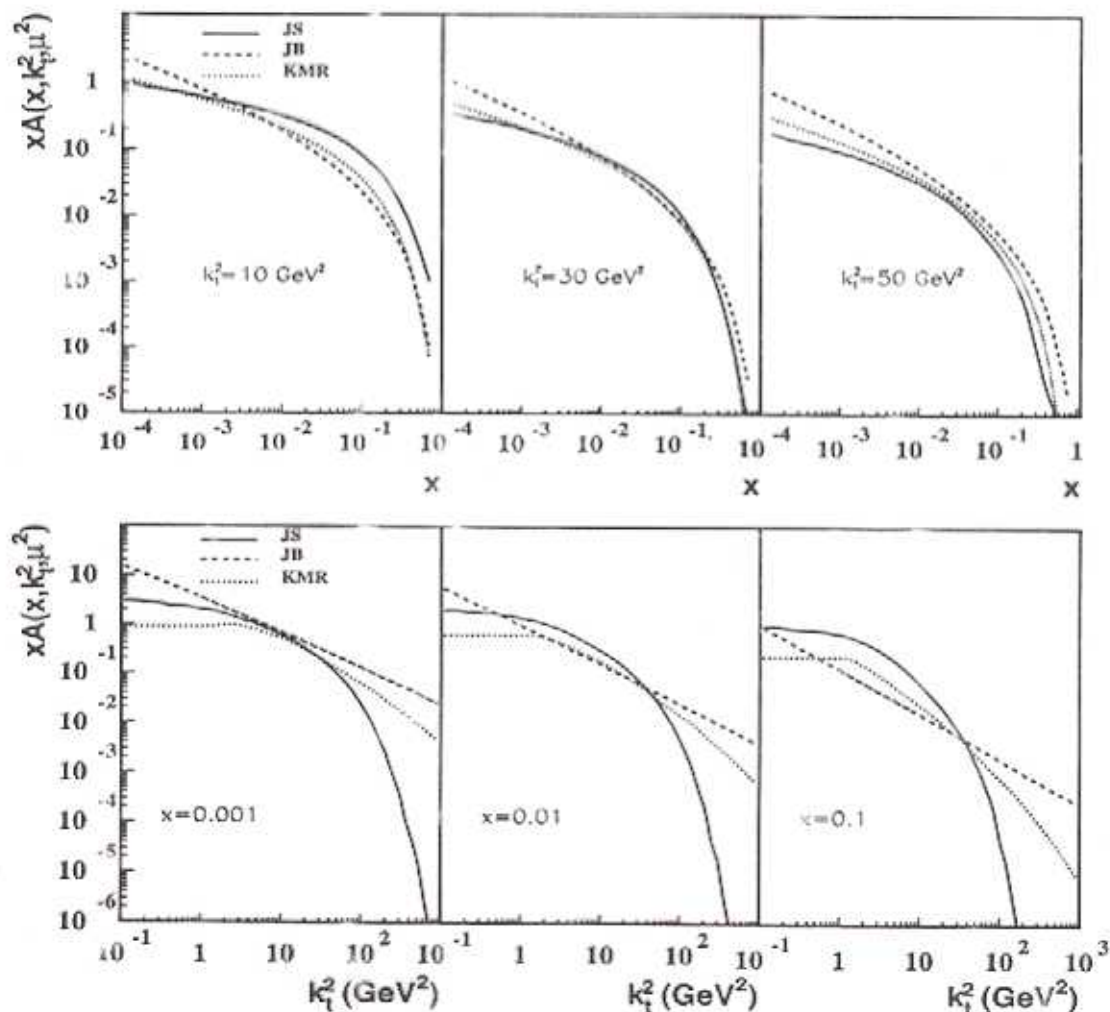

Figure 2: *The k_t dependent (unintegrated) gluon density at $\mu^2 = 100$ GeV^2 as a function of x for different values of k_t^2 (upper part) and as a function of k_t^2 for different values of x (lower part) as given by JS [22,23] (solid line), JB [37] (dashed line) and KMR [38,42] (dotted line).*

From Fig. 2 we see that all three unintegrated gluon distributions show a significantly different behavior as a function of x but even more as a function of k_t. It will be interesting to see, how this different behavior is reflected in the prediction of cross sections for experimentally observable quantities as charm production at HERA.

It is also interesting to consider the limit $k_t \to 0$ of the matrix elements. To do that we define a reduced cross section $\tilde{\sigma}$:

$$\tilde{\sigma}(k_t) = \int d\text{Lips}\, |ME|^2 \tag{5}$$

where we integrate over the Lorentz-invariant-phase-space (Lips) of the final state quarks. The matrix element $|ME|^2$ is taken from CE-CCH, where we have set $16\pi^2 \alpha_{cm} \alpha_s e_q^2 \equiv 1$. In Fig. 1
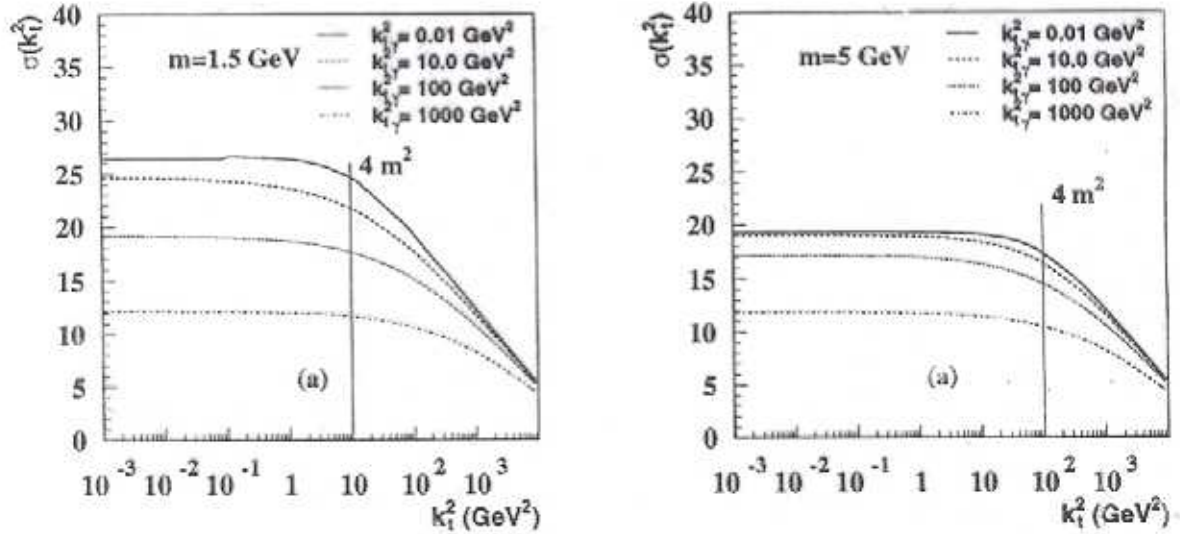

Figure 1: *The reduced cross section $\tilde{\sigma}(k_t)$ as a function of the transverse momentum k_t of the incoming gluon for different values of the transverse momentum of the incoming photon $k_{t\gamma}$ ($m = 1.5$ GeV in (a), $m = 5$ GeV in (b), $\sqrt{s} = 30000$ GeV and a fixed $x_\gamma = x_g = 0.01$).*

we show $\tilde{\sigma}(k_t)$ as a function of the transverse momentum of the incoming gluon k_t for quark masses of $m = 1.5$ GeV in Fig. 1a and for $m = 5$ GeV in Fig. 1b using $\sqrt{s} = 30000$ GeV and a fixed $x_\gamma = x_g = 0.01$. In both cases a smooth behavior for $k_t \to 0$ is observed. It is also interesting to note that in all cases the cross section starts to decrease at $k_t^2 \gtrsim 4m^2$. The region

4

3.2 Transverse momentum distribution of D^* mesons: sensitivity to unintegrated gluon distributions
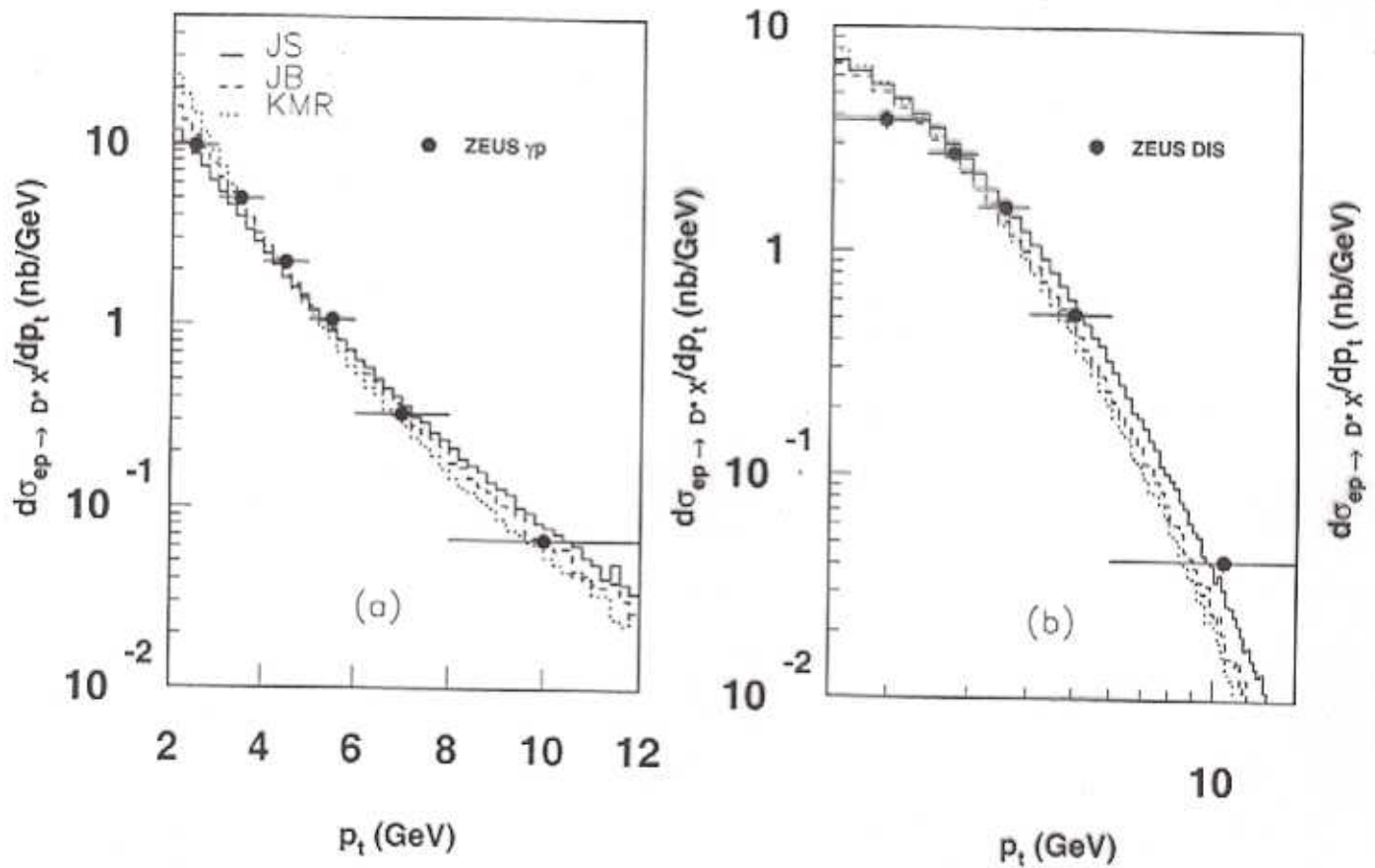

Figure 4: *The differential cross section $d\sigma/dp_t$ for D^* production: (a) in photo-production (ZEUS [44]), (b) in DIS (ZEUS [45]) and (c) in DIS (H1 [46]). The solid (dashed, dotted) line corresponds to using the JS (JB, KMR) unintegrated gluon density (all calculated at parton level with Peterson f.f.)*

In spite of differences are observed in the X_g and K_t distributions between the different u.g.d. (see Fig.2), very similar predictions for D^* c.s. as a function of the t.m. p_t are obtained.

SHA results for
D^* in DIS

for ZEUS kinematic region:

$$1 < Q^2 < 600 \text{ GeV}^2$$

$$0.02 < y < 0.7$$

$$1.5 < p_T(D^*) < 15 \text{ GeV}$$

$$|\eta(D^{*\pm})| < 1.5$$

- <u>Comparison of parton and hadron level</u>:

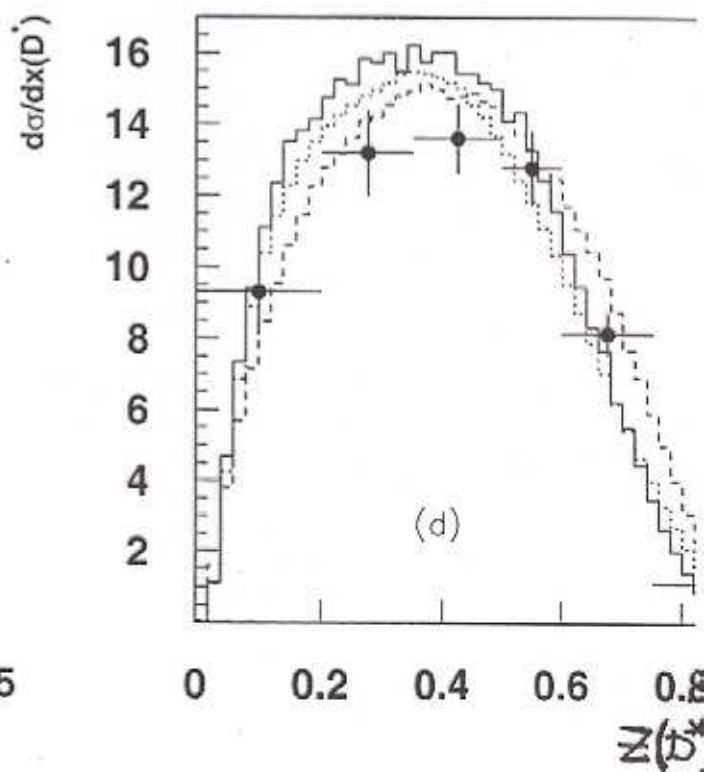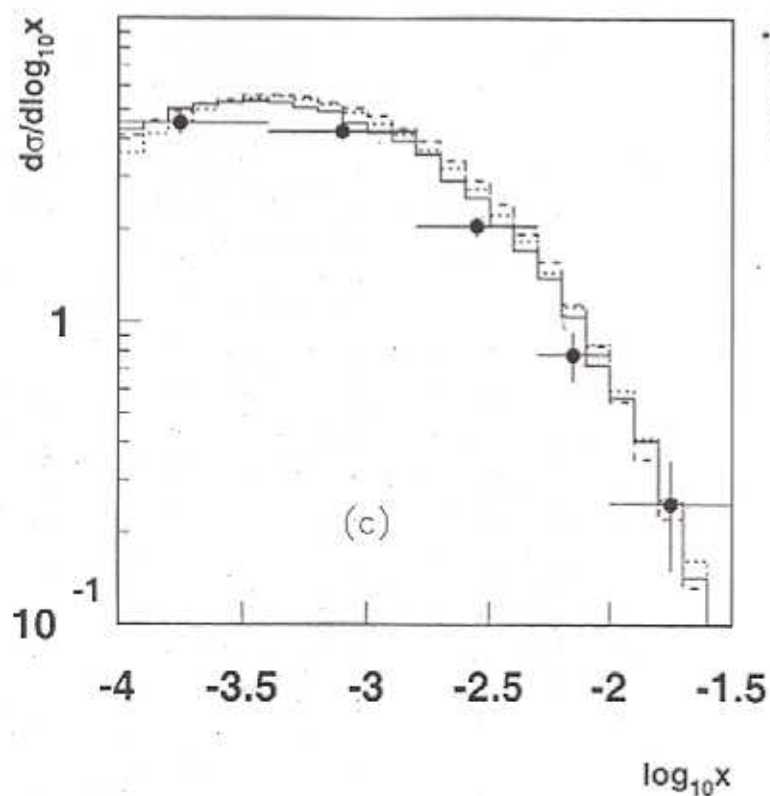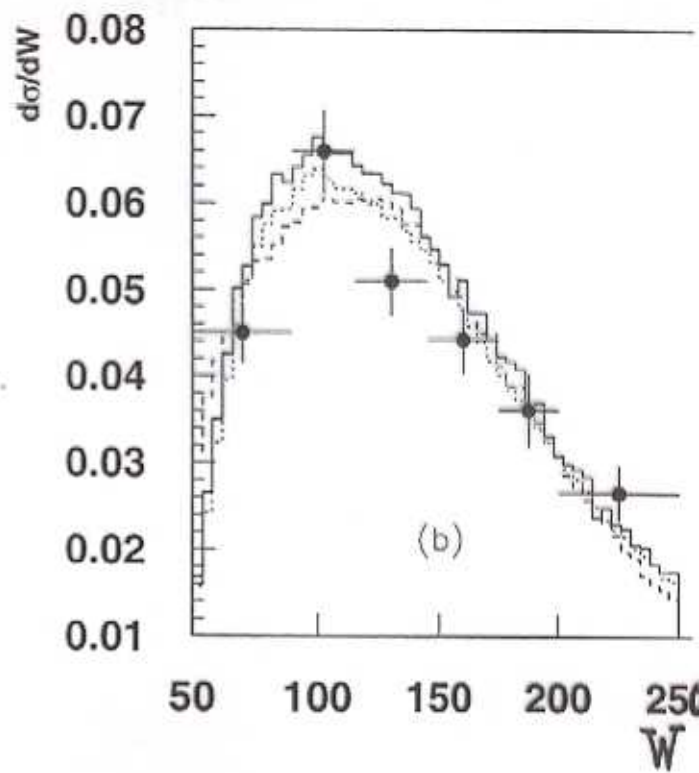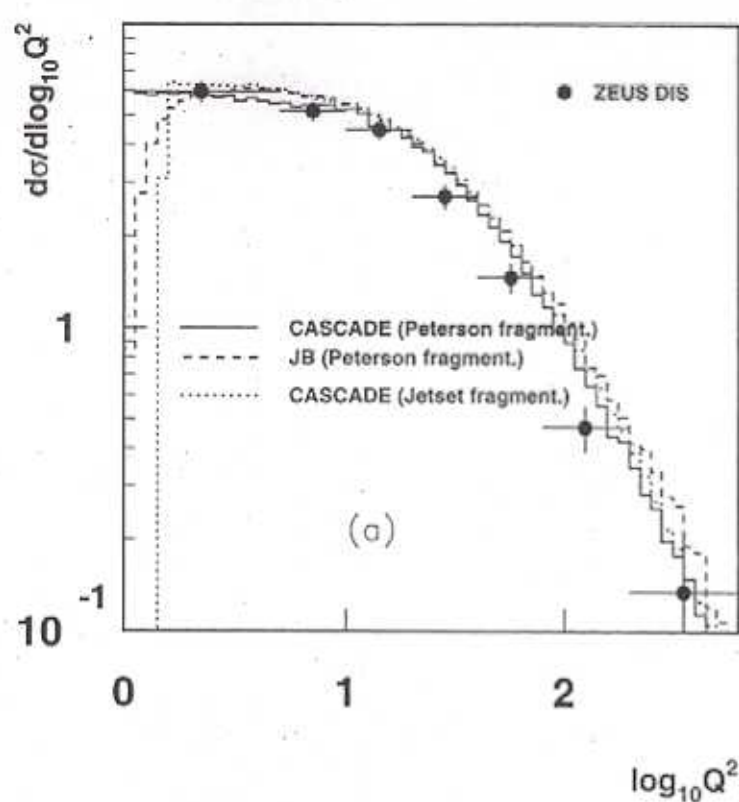Q_0^2, W, x_{Bj} and z_{D^*} distributions

Fig. 6: Differential c.s. of D^* in DIS. Shown is a comparison of the calculations using CASCADE (with JETSET/PYTHIA charm f.f.) and JS (solid line), and JB (dashed line) u.g.d.

4. Rapidity distribution of D* mesons: comparison of parton and hadron level

In photoproduction and DIS the __d.c.s. $d\sigma/d\eta$__ (η-pseudorapidity of the D* meson) __is sensitive to the choice of the u.g.d.__ (Fig. 7)
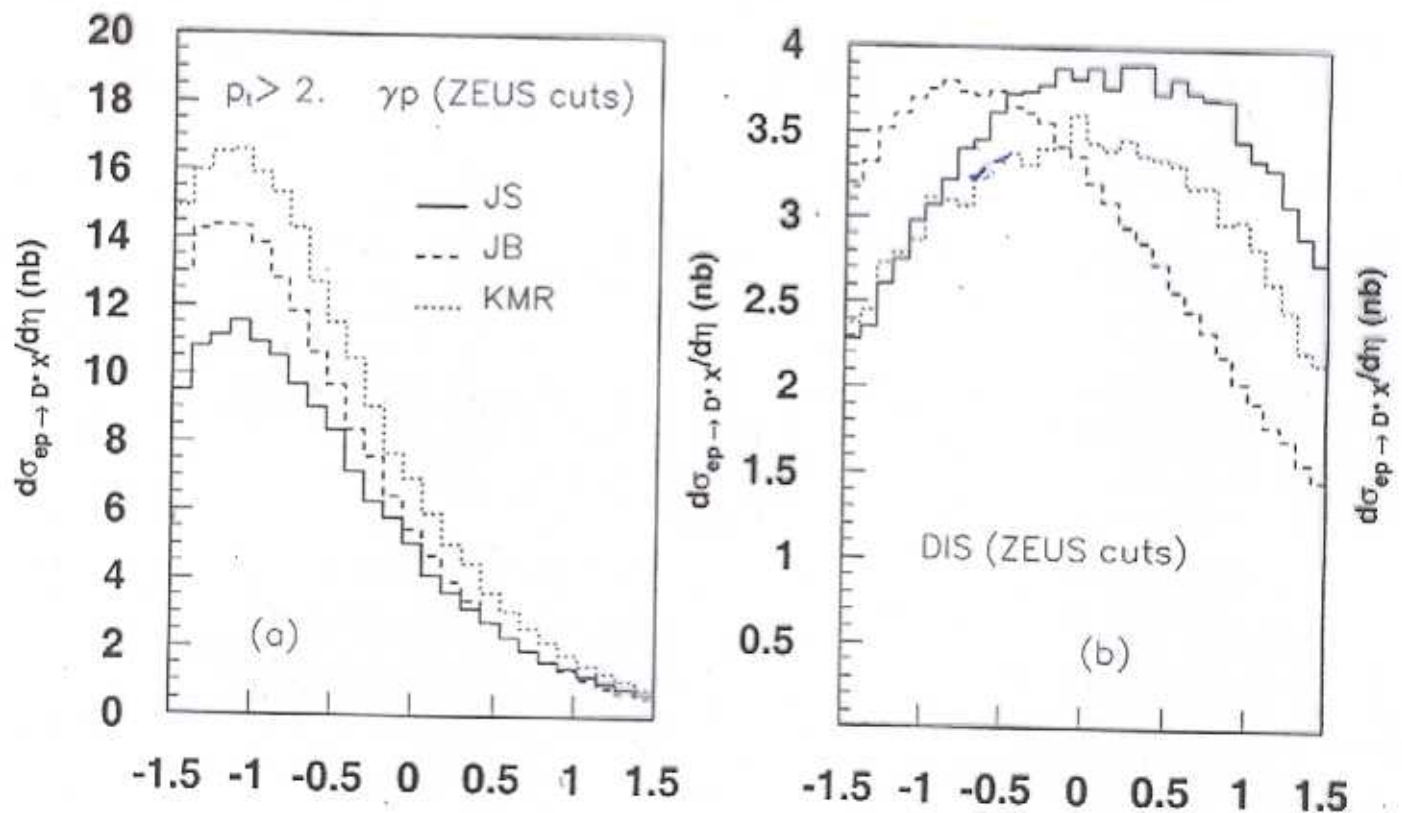

Fig. 7: The d.c.s. $d\sigma/d\eta$ for D* production.

⟹ Large differences in $d\sigma/d\eta$ are visible,

(but)

the η distr. is __also sensitive to the__ $c \to D^*$ __fragmentation__ and therefore a clear distinction of the u.g.d. based on this quantity alone might be questionable.
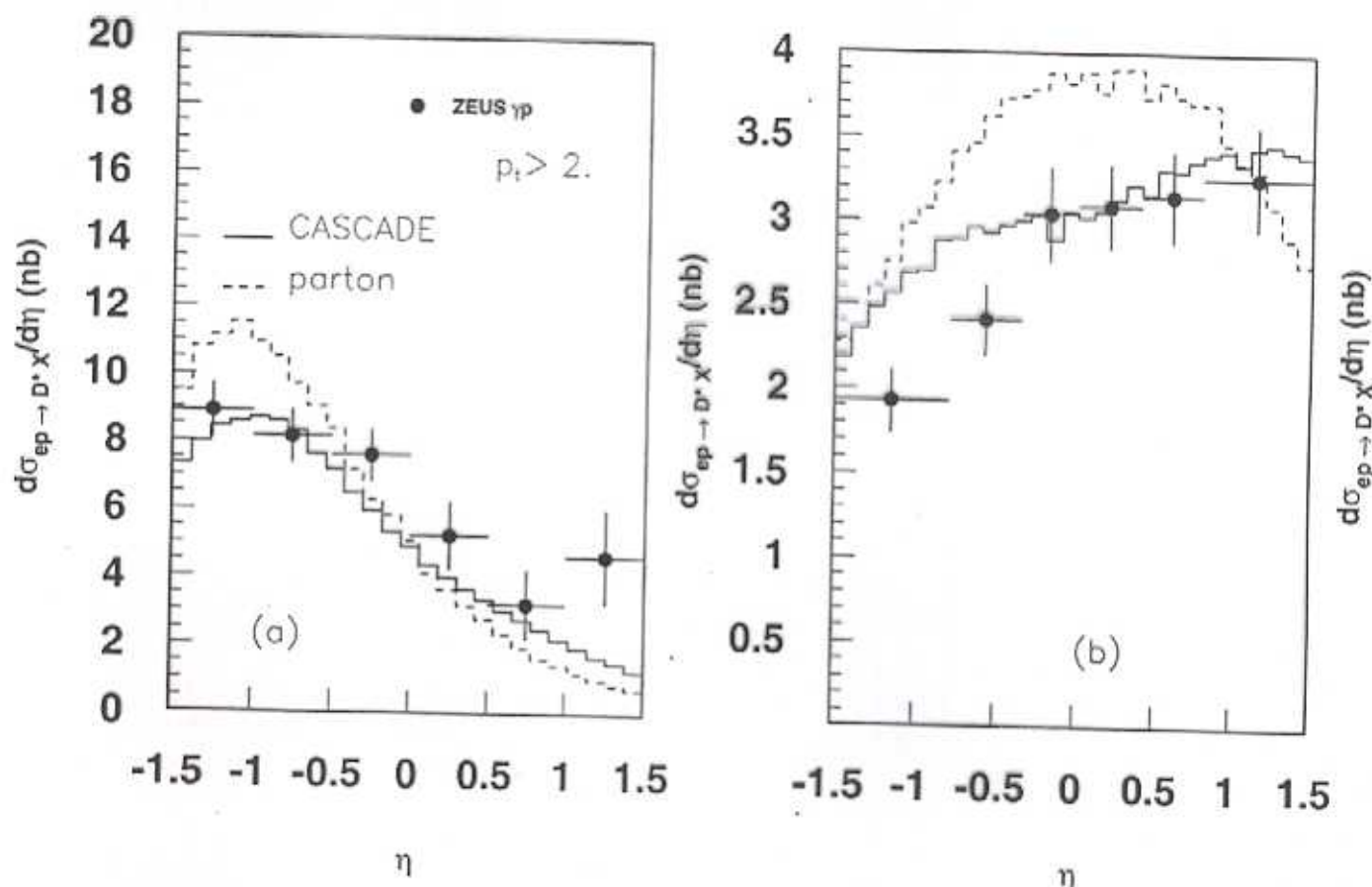
It is seen in Fig. 8

Figure 8. *The differential cross section dσ/dη for D* production: (a) in photo-production as mea-sured by ZEUS[44], (b) in DIS (ZEUS[45]) and (c) in DIS (H1[46]). Shown is a comparison of the parton level calculations using the JS (dash. line) full hadron level simulation from CASCADE (solid line) with exp. data. unintegrated gluon density and the*

⟹ The parton level prediction with the Peterson f.f. is not able to describe the data over the full range of η (dashed lines).

• The effect of <u>full hadron level simulation is clearly visible</u> as CASCADE gives a much better discription of the data.

(But)

• <u>in photoproduction</u> even <u>the full event simulation of CASCADE shows differences to the data</u> at <u>large η>1.</u>

5. D^* and associated jet production: comparison of parton and hadron level.

ZEUS Collaboration has measured charm and associated jet production

$$ep \rightarrow e^\# D^*_{+2jets} + X$$

J. Breitweg et al.,
Eur. Phys. J. $\underline{C6}$ (1999) 67

In these measurements, the quantity of interest is x_γ^{OBS} _the fractional photon momentum_ involved in _the production of the two jets of highest_ E_t, which experimentally is defined as

$$x_\gamma^{OBS} = \frac{E_{1t} e^{-\eta_1} + E_{2t} e^{-\eta_2}}{2 E_e y}$$

with E_{it} and η_i being the transverse energy and rapidity of the hardest jets, y being the fractional photon energy

In the BFKL and/or CCFM equations the transverse momenta of the exchanged or emitted partons are only restricted by kinematics. In such a scenario the hardest p_t emission can be anywhere in the gluon chain and needs not to sit closest to the photon as required by the strong q^2 ordering in DGLAP.

In photoproduction charm quarks are predominantly produced via $\gamma \to c\bar{c}$

The observation of any emission (jet) with $p_t > p_t^c$ $(p_t^{\bar{c}})$ indicates a scenario, which in DGLAP is possible only in a full $O(\alpha_s^2)$ calculation (or when charm excitation of the photon is included).

However, in k_t factorization such a scenario comes naturally, since the transverse momenta along the evolution chain are not k_t ordered.

$x_\gamma \sim 1$ $x_\gamma < 1$

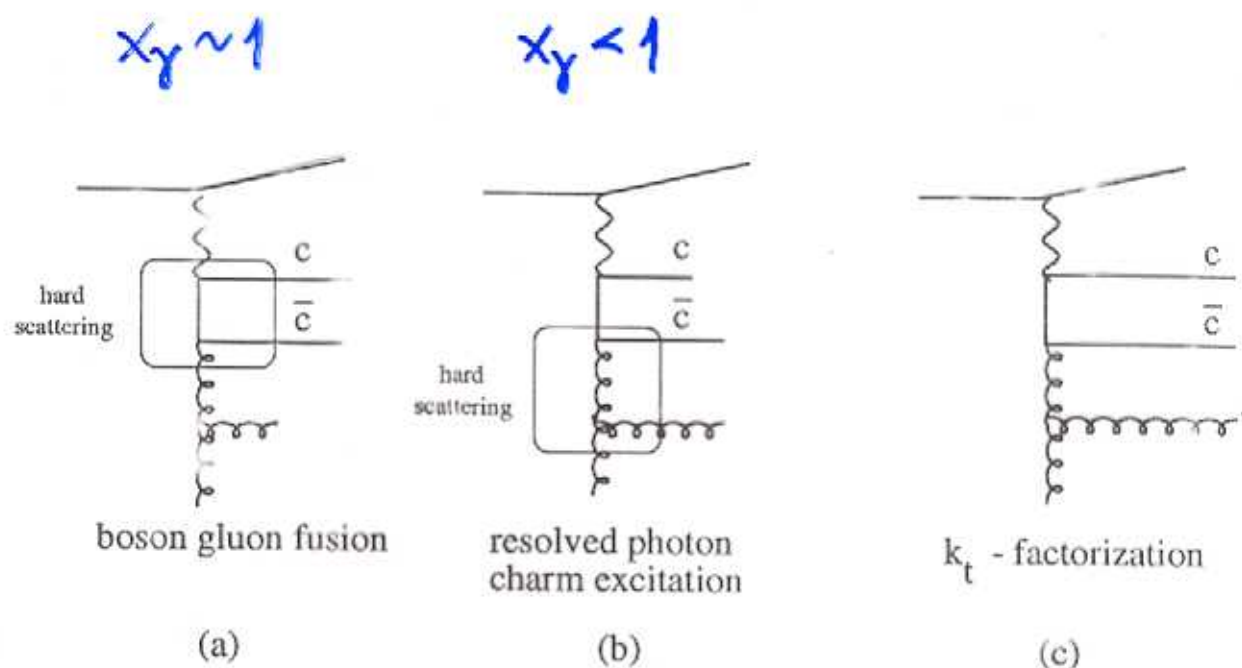| boson gluon fusion | resolved photon charm excitation | k_t - factorization |
| (a) | (b) | (c) |

Figure 11: *Diagrammatic representation of the processes involved in charm photoproduction. (a) shows the typical boson-gluon fusion diagram, the hard partons are the $c\bar{c}$ quarks. (b) shows a typical resolved photon (charm excitation) diagram, the hard parton are here the $\bar{c}g$. (c) shows a typical diagram in k_t-factorization, any two of $c\bar{c}g$ can be the hardest partons.*

Thus, if the two hardest t.m. jets are produced by the $c\bar{c}$ pair, then x_γ^{OBS} is close to unity (Fig. 11a)

But if a gluon from initial state cascade together with one of the c-quarks form the hardest t.m. jets, then $x_\gamma^{OBS} < 1$ (Fig. 11b). It is <u>resolved photon</u> like process in LO collinear approximation.

Such a scenario is obtained naturally also in a full NLO ($\sim \alpha_s^2$) calculation, because in the three parton final state ($c\bar{c}g$) any of these partons are allowed to take any kinematically accessible value (Fig. 11c)

In <u>the SHA</u> the anomalous component of the γ ($\gamma \to c\bar{c}$) is automatically included, since there is <u>no restriction on the t.m. along the evolution chain.</u>

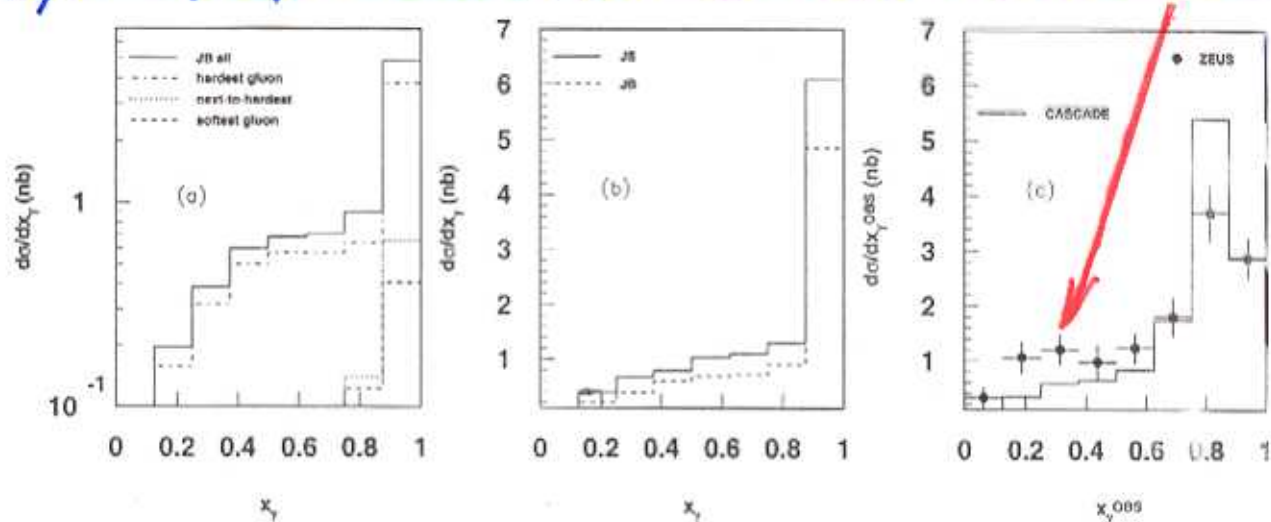a) <u>Exp. x_γ spectrum</u> (Fig. 12c) shows a <u>tail to small x_γ</u>.

Figure 12: The differential cross section $d\sigma/dx_\gamma$ for $Q^2 < 1\ GeV^2$. In (a) the parton level calculation is shown using the JB unintegrated gluon density (solid line). Shown are also the contributions where the gluon takes the largest (dash-dotted line), next-to-largest (dashed line) and smallest (dotted line) transverse momentum. In (b) the JB (solid line) and JS (dashed line) sets are used in the parton level calculation. In (c) the measurement of ZEUS [44] is compared to the full event simulation obtained from CASCADE using the JS unintegrated gluon distribution.

It means that <u>the hardest emission is indeed not always coming from the c-quarks</u>.

In <u>Fig. 12a</u> we see that a significant part of the c.s. comes from events, where the gluon is the jet with the largest transverse moment

<u>Fig. 12b</u>: the details depend on the u.g.d.

<u>Fig. 12c</u>: the full event simulation of CASCADE at hadron level.

⟹ SHA effectively simulates c-quark excitation and indeed the hardest p_t emission comes frequently from a gluon in the initial state gluon cascade. (Fig. 11c).

b) The angular distribution of <u>resolved photon like</u> events $(x_\gamma < 0.75)$ compared to the <u>direct photon like</u> events $(x_\gamma > 0.75)$.

An important difference between the two (direct-Fig.11 and resolved - Fig.11b) processes: a quark is the propagator in first case and a gluon is in second one.
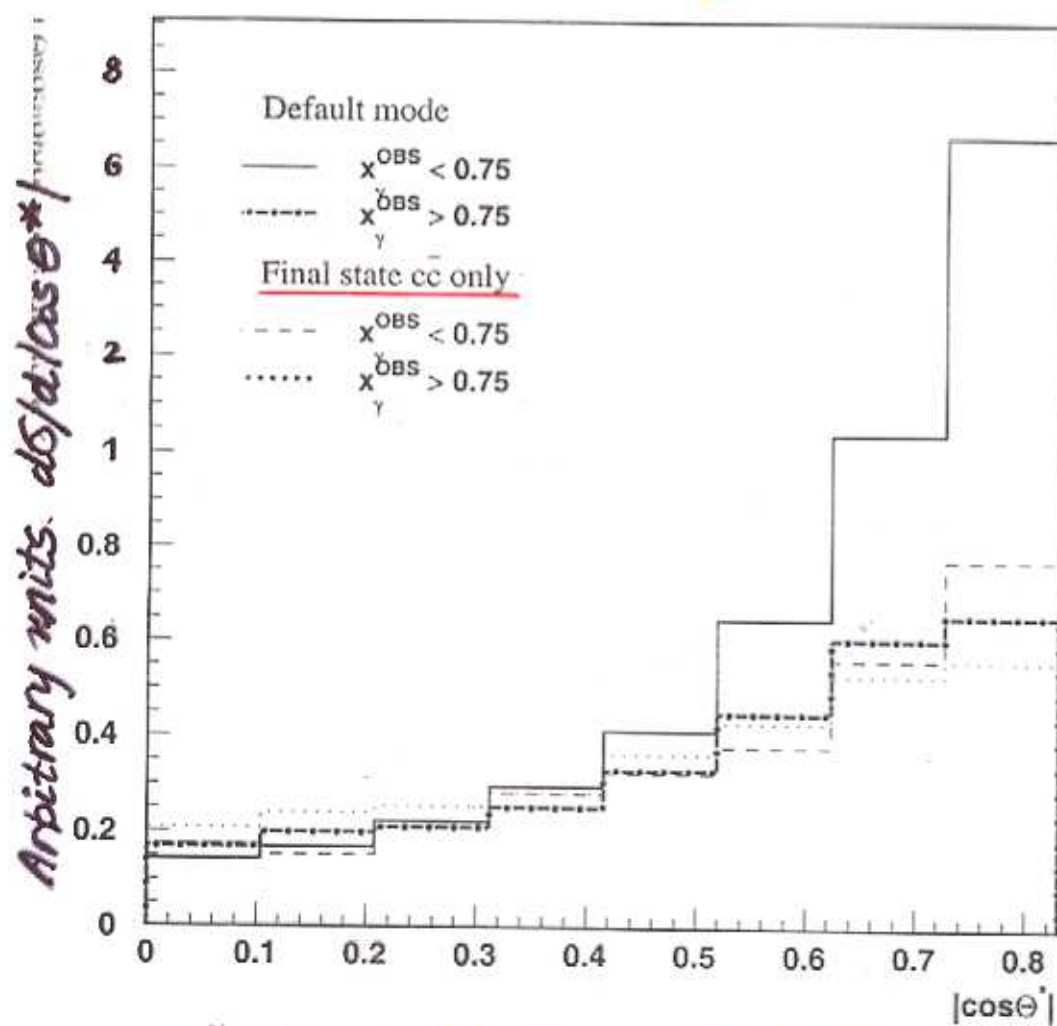
The a.d. of dijets with b^* in the f.s. is dependent on the type of propagator $(q$ or $g)$ connecting both jets.

In the collinear approx the a.d. is determined by the m.e.:

$\gamma g \to c\bar{c}$ in the direct case

$cg \to cg$ in the r. case

<u>In SHA</u> the a.d. will be determined from off-shell m.e. which covers both scattering processes

Arbitrary units. $d\sigma/d|\cos\theta^*|$

8
6
4
2
1
0.8
0.6
0.4
0.2
0

Default mode

——— $x_\gamma^{OBS} < 0.75$

-·-·- $x_\gamma^{OBS} > 0.75$

<u>Final state $c\bar{c}$ only</u>

- - - $x_\gamma^{OBS} < 0.75$

······ $x_\gamma^{OBS} > 0.75$

0   0.1   0.2   0.3   0.4   0.5   0.6   0.7   0.8

$|\cos\theta^*|$

θ^* - the scattering angle of the hard jets to the beam axis in the dijet c.m.s.

We see <u>the direct photon like events</u> give a slow rise in c.s.

The c.s. of the <u>resolved photon like events</u> rises <u>very rapidly</u> because of the t-channel gluon exchange being a combined effect the off-shell gluon and u.g.d.

! <u>By only allowing the final state partons $(c\bar{c})$ to appear</u>
! we should expect to see only the g-exchange kind of behavior for both direct and resolved like events.

In order to futher probe the parton dynamics in SHA, we divide the entire sample into two parts, one where D* proceeds the γ direction ($z_{D*} < 0$) and one where it travels along the proton direction ($\eta_{D*} > 0$). If t-channel gluon is the dominant contribution to q then the a. d. will be peaked towards the incoming photon direction.

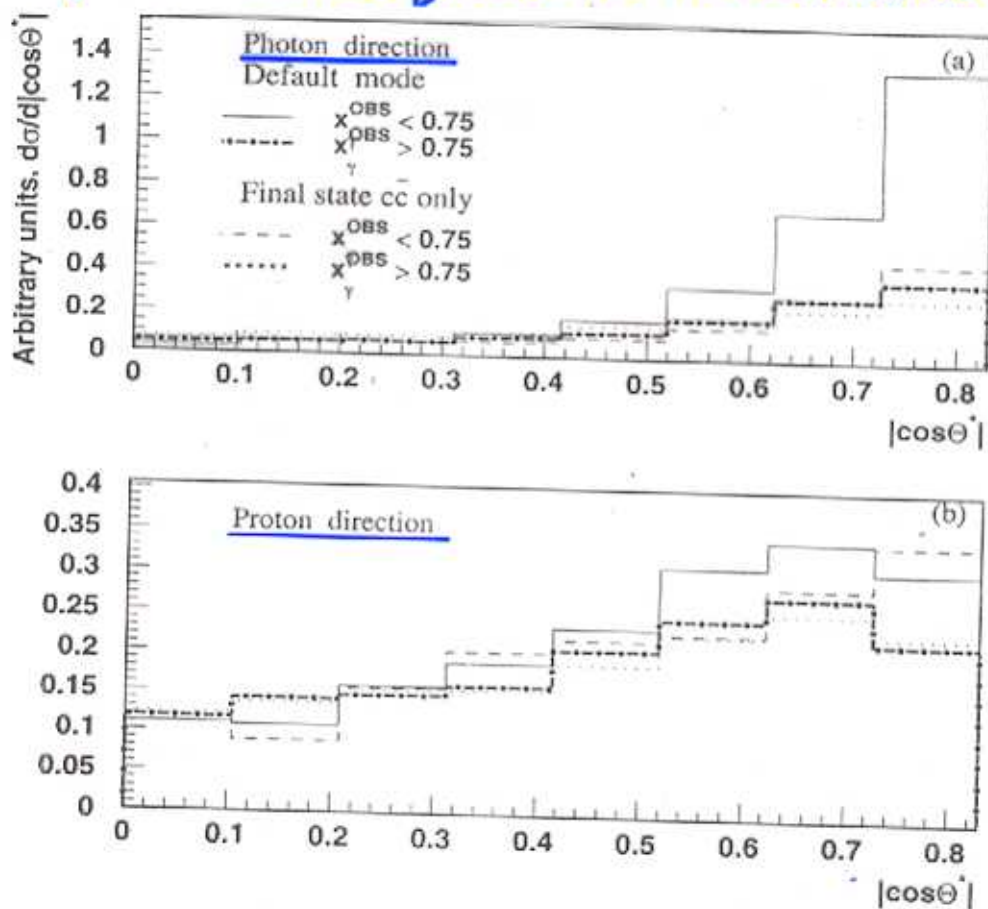

Figure 14: $|\cos\theta^*|$ distribution with $\eta_{D^*} < 0$ (a) (photon direction) and $\eta_{D^*} > 0$ (b) (proton direction) within the kinematic range of the ZEUS measurement [50,51]

In the case of D* in the photon direction there is a steep rise in the c.s. for resolved photon like events compared to the direct photon like evens (Fig. 14a)
⟹ „Charm excitation" is properly simulated through the initial state gluon cascade in the SHA

For the D* in the proton direction we see only a mild rise in c.s. for both direct and resolved photon like events (Fig. 14b)
⟹ the quark exchange is the dominant contribution.

Conclusion

Three different models based on small x resummation (BFKL and CCFM) and K_t factorization have been studied:
1) on _parton level_ (JB and KMR)
2) on complete simulation of the initial state parton shower and hadronisation (MC _CASCADE generator_ with JS u.g.d.)

The aim has been to find optimal sets of model parameters for description all charm HERA data.

It was observed:

① Although the different u.g.d. exhibit different behaviors as a function of x but especially K_t we find good agreement the results with data on $p_t, \log Q^2, \log W, \log X_{Bj}$. distributions

These variables are not sensitive to details of SHA

2) The _z_D distr._ may be due to different treatment of the D^* fragmentation

3) The _η distr._ needs a full simulation of the initial state parton emission and hadronization

④ In photoproduction of $D^* +$ jets _a gluon from the initial cascade frequently produces the jet of highest p_t_